Monte Carlo simulations of electronic excitation transfer in polymer composites and comparison to theory

D. M. Hussey, S. Matzinger, and M. D. Fayer
Department of Chemistry, Stanford University, Stanford, California 94305-5080

(Received 22 April 1998; accepted 13 August 1998)

Monte Carlo (MC) simulations of electronic excitation transfer (EET) among a small number of chromophores covalently incorporated into copolymer molecules are presented and used to test the results of previously developed analytical EET theories that are useful for the study of polymer chain structure [K. A. Peterson and M. D. Fayer, J. Chem. Phys. **85**, 4702 (1986)] and phase separation in polymer blends [A. H. Marcus and M. D. Fayer, J. Chem. Phys. **94**, 5622 (1991)]. The simulations and theory account for EET among chromophores bound to a single chain and among chromophores attached to different chains. The calculated quantity, $\langle G^s(t)\rangle$, which is the probability that an initially excited chromophore is still excited at time t, is related to time-resolved fluorescence depolarization experiments. The theories, particularly the treatment of interchain EET, depend on a series of approximations whose efficacy has not been determined. Close agreement between the MC simulations and the analytical theory are found for a variety of situations, including those that mimic real polymer systems. The limits beyond which agreement is weakened provide specific guidelines for the design of polymer structure and phase-separation experiments. © *1998 American Institute of Physics.* [S0021-9606(98)52343-4]

I. INTRODUCTION

The desire to understand the structures and phase behaviors of polymer composites has motivated a great deal of research.[1–3] Because polymeric melts and glasses have a fascinating array of characteristics that distinguish them from small-molecule liquids and solids, they are of great interest both as versatile industrial materials and as model systems for scholarship in physics, chemistry, biology, and engineering. In particular, polymer composites have a vast repertoire of phase behaviors which confer upon them a variety of architectures at the molecular level, corresponding to a wide range of bulk physical properties.

The theories developed over a number of years for calculating the time-resolved observables measured in optical studies of electronic excitation transfer (EET) (Refs. 4–14) apply to systems of random copolymers,[4,6,15–18] micelle surfaces,[5,19,20] and the micellar, lamellar, and cylindrical phases of diblock copolymers,[7,8] making it possible to probe the architecture of a variety of polymer composites at the molecular level. Since the measurement of EET can involve the detection of single fluorescent photons, EET experiments afford a sensitivity that permits probing the configurations of copolymers which are present in a composite at very low concentrations.

Random copolymers consisting of optically inert monomers and a small number of fluorescent chromophores are blended with an optically inert host material to obtain the experimental system. Fluorescent chromophores transfer electronic excitations through nonradiative resonant dipolar interactions between excited and unexcited chromophores, as described by Förster.[21] This interaction is parameterized by the Förster distance, R_0, at which the rate of transfer to unexcited chromophores is equal to the fluorescence decay rate of the donor in the absence of acceptors. For common chromophores, R_0 is between 5 and 60 Å. The sensitivity of Förster transfer to the distance between chromophores is dependent upon this single parameter, which can be determined spectroscopically[21] or with transfer experiments.[22,23] Because Förster transfer is strongly distance-dependent, falling off as $1/r^6$, where r is the chromophore separation, EET observables contain information about chromophore spatial distributions.

EET has been modeled such that a calculable quantity, $G^s(t)$, emerges.[9] $G^s(t)$, which is readily compared with experimental observables, is the diagonal, or ''self'' part of the Green function solution to the Pauli master equation.[9,10] It is the probability that an excitation is on an initially excited chromophore at time t, either because the excitation has not been transferred to another chromophore, or because it has been transferred away from and returned to the initially excited chromophore. Since the time-dependence of the observable arises from the spatial distributions of unexcited chromophores around the ensemble of excited chromophores, the ensemble-average of $G^s(t)$ is the quantity of interest.

If EET occurs among identical chromophores that can continually transfer excitations, the system is donor–donor, or DD. In a DD experiment, polarized light excites a very small fraction of the chromophores, preferentially exciting those oriented so that the light's electric field has a large projection along the absorption dipole. Excitation transport occurring among chromophores with randomly oriented dipoles results in loss of the polarization anisotropy of the ensemble of excited chromophores. A time-resolved fluorescence anisotropy decay, $r(t)$, which is related[11] to $\langle G^s(t)\rangle$, is measured. The experimental determination of $\langle G^s(t)\rangle$ pro-

vides information about the spatial distribution of chromophores, and therefore about polymer structure.

The analytical theory for *intra*chain EET (Ref. 4) depends on a series of approximations, including a cumulant expansion truncated to first order based on a two-particle approximation that greatly simplifies the numerical calculation of observables.[4,12,13] In previous work, the intrachain theory allowed the ensemble-average radius of gyration of copolymer molecules present at low concentrations in optically inert hosts to be determined with time-resolved anisotropy decay measurements.[4,15,16]

When copolymer molecules are in close proximity, as in the process of phase-separation, the theory can also be used to determine the contribution of *inter*chain EET to the observable.[5] The theory for interchain transfer relies on additional assumptions, including the independence of intrachain and interchain contributions to the total observable, and the Effective Chromophore Method, which entails a renormalization of the problem resulting in the treatment of entire chromophore-bearing copolymers as though they were each, effectively, single chromophores. Effective chromophores have transport dynamics that depend upon the nature of the copolymer chains they represent, and permit the reduction of the problem from the interactions of many chromophores on different chains to the pairwise interactions of effective chromophores. Experimental systems exist for which the interchain transfer theory may be useful.[6,17,18] However, the influence of the assumptions on the accuracy of the theoretical calculations has not been tested.

The purpose of this paper is to test the assumptions made in the theoretical developments describing both intra- and interchain excitation transport dynamics with the aid of MC simulations. The results of detailed simulations of EET in various systems show excellent agreement between simulation and experiment for intrachain EET and reasonable agreement for interchain transport. The simulations provide insights into the experimental conditions for which EET provides a useful probe of polymer structure and phase separation.

II. OUTLINE OF THE THEORY

The general expression for $\langle G^s(t)\rangle$ for an initially excited donor (chromophore 1) and $N-1$ excitation acceptors (chromophores 2) in an ensemble of N chromophores in a restricted volume is[4]

$$\langle G^s(t)\rangle = \frac{1}{V_1}\int_{\text{space}} \exp\left\{\left(\frac{N-1}{2V_2}\right) \times \int_{\text{space}} \left\{\exp\left[\left(\frac{-2t}{\tau}\right)\left(\frac{R_0}{r_{12}}\right)^6\right]-1\right\} u(\mathbf{r}_2)\,d\mathbf{r}_2\right\} \times u(\mathbf{r}_1)\,d\mathbf{r}_1, \tag{1}$$

where $u(\mathbf{r})$ is a function representing the spatial distribution of chromophores. For spherical symmetry, the vector nature of the average is equivalent to having a factor of $4\pi r^2 dr$ with $|\mathbf{r}|=r$, so $u(\mathbf{r})=1$ for a random distribution. V is the volume spanned by the chromophore distribution. The normalization condition requiring that all of the chromophores in a particular distribution be found in the volume occupied by the distribution is written, $\rho\int_{\text{space}} u(\mathbf{r})\,d\mathbf{r}=N-1$, where ρ is the number density of chromophores. r_{12} is the distance between chromophores 1 and 2. Chromophores other than chromophore 1 are called acceptors, even though they are identical to chromophore 1 and can transfer excitations back to chromophore 1 as well as among themselves. The inner integral is performed over all possible positions of excitation acceptors, and the outer integral is performed over all possible positions of the initially excited chromophore.

Equation (1) is based on the work of Huber,[12] who developed a treatment of EET among randomly distributed chromophores in an infinite volume using a cumulant expansion. Use of a two-particle approximation derived by Blumen[13] allowed truncation of the cumulant expansion after the first-order term. Peterson and Fayer[4] demonstrated that Huber's $\langle G^s(t)\rangle$ produced results matching those from the infinite-order diagrammatic expansion method of Gochanour, Andersen, and Fayer.[9] They modified Huber's method to construct expressions for $\langle G^s(t)\rangle$ for chromophores in finite-volume, nonrandom geometries, e.g., the Gaussian segment-distributions of polymer chains. They showed that for a finite number of chromophores in a spherical volume, their model was slightly less accurate than that based on a second-order density expansion with a Padé approximant.[11,14]

The cumulant expansion method has a number of advantages over the density expansion method and the infinite-order diagrammatic theory. The diagrammatic approach requires translational invariance of the ensemble average around the point of initial excitation as well as the ability to pass to the thermodynamic limit. Neither of these conditions is applicable to finite-volume, spatially inhomogeneous systems. In contrast to the cumulant treatment, the density expansion involves equations in Laplace space, making comparisons between experiment and theory more difficult. Furthermore, to achieve reasonable accuracy, it is necessary to perform the density expansion to second order (three particles). Obtaining the second-order result for complex geometries is difficult.

To test the approximations inherent in the general form of Peterson and Fayer's expression for EET as distinct from their specific model of a polymer chain, MC simulations are first compared to expressions for EET between chromophores randomly distributed in a three-dimensional Gaussian cloud,[7]

$$\langle G^s(t)\rangle = 4\pi\left(\frac{3}{2\pi\sigma^2}\right)^{3/2}\int_0^{r\max}\exp\left(\frac{-3r_1^2}{2\sigma^2}\right)\exp\left\{\pi(N-1) \times\left(\frac{3}{2\pi\sigma^2}\right)^{3/2}\int_0^{\pi}\int_0^{r\max}\exp\left(\frac{-3r_2^2}{2\sigma^2}\right)\left(\exp\left[\left(\frac{-2t}{\tau}\right) \times\left(\frac{R_0}{r_{12}}\right)^6\right]-1\right) r_2^2\,dr_2\,\sin\theta_2\,d\theta_2\right\} r_1^2\,dr_1, \tag{2}$$

where $r_{12}=r_1^2+r_2^2-2r_1r_2\cos\theta_2$, and σ is the standard deviation of the Gaussian. In the three-dimensional Gaussian cloud problem, the ensemble-average chromophore distribu-

tion has a maximum at the center and falls off in a three-dimensional Gaussian manner. The ensemble average is over all configurations of donor and acceptor chromophores arrayed in this Gaussian manner. The equivalent problem for chromophores randomly distributed in a sphere is examined in Ref. 24.

We also examine the behavior of $\langle G^s(t)\rangle$ for chromophores inside a sphere with the initially excited chromophore at the center of the sphere. Then, the average over positions of the initially excited chromophore is removed,

$$\langle G^s(t)\rangle = \exp\left\{ 2\pi(N-1)\left(\frac{3}{4\pi r^3}\right) \times \int_0^r \left(\exp\left[\left(\frac{-2t}{\tau}\right)\left(\frac{R_0}{r_{12}}\right)^6\right] - 1\right) r_2^2 dr_2 \right\}. \quad (3)$$

As the volume becomes very large, $\langle G^s(t)\rangle$ should converge to the analytical expression for $\langle G^s(t)\rangle$ in a random, infinite, three-dimensional solution of chromophores[25,26]

$$\langle G^s(t)\rangle = \exp\left[\frac{-4\pi c}{3}\left(\frac{t}{\tau}\right)^{1/2} R_0^3 (2^{1/2})\Gamma\left(\frac{1}{2}\right)\right], \quad (4)$$

where c is the number density of chromophores, and Γ is the complete gamma function.

Peterson and Fayer modeled polymer chains using a segmental distribution function related to one described by Yamakawa,[27] which yields a Gaussian distribution of segment density for the ensemble average. The statistical segment length, a, is set to the Kuhn length,[28] which can be determined experimentally with light scattering[29] or as described in Ref. 4. The distribution of chromophores on these chains is identified with that of the chain segments, and a factor accounting for the presence of an acceptor chromophore which may be on the same segment as the initially excited chromophore is added. EET calculations using this model [Eq. (5)] and the cumulant method are compared with the simulated chromophore-bearing polymer chains below,

$$\langle G^s(t)\rangle = \frac{1}{N}\sum_{i=1}^{\bar{N}} \left\{ \exp\left\{ \frac{4\pi}{2} \int_0^\infty [np'(r_{12}) + (N-1-n)p_i(r_{12})] \times [\exp(-2\omega_{12}t)-1] r_{12} dr_{12} \right\}\right\}, \quad (5a)$$

with

$$p'(r_{12})dr_{12} = 4\pi r_{12}^2 dr_{12}, \quad 0 \leqslant r_{12} \leqslant (a/2); \quad = 0, \quad r_{12} > (a/2); \quad (5b)$$

$$p_i(r_{12})dr_{12} = \frac{4\pi}{N-1}\sum_{\substack{j=1 \\ j\neq i}}^{\bar{N}} \left(\frac{3}{2\pi a^2 |i-j|}\right)^{3/2} \times \exp\left(\frac{-3r_{12}^2}{2a^2|i-j|}\right) r_{12}^2 dr_{12}, \quad (5c)$$

and $\omega_{12} = (1/\tau)(R_0/r_{12})^6$. ω_{12} is the transfer rate constant. The likelihood of having an additional chromophore on a given segment is $n = (N-1)/\bar{N}$, where $\bar{N}$ is the number of statistical segments per copolymer molecule. The distribution of additional chromophores on a segment around the center of that segment is p', and p_i is the configuration-averaged radial probability of finding any other polymer segment, j, a distance away from a segment i.

Marcus and Fayer[5] treated the problem of calculating $\langle G^s(t)\rangle$ for EET among chromophores on the surfaces of a random distribution of spheres, and extended the treatment to apply to EET among chromophores on multiple polymer chains modeled as Gaussian clouds.[6] This development depends upon the separability of $\langle G^s(t)\rangle$ into independent components, $\langle G^s_{\text{on}}(t)\rangle$, which is the result of Eq. (5) and represents EET among only those chromophores on the same copolymer molecule, and $\langle G^s_{\text{off}}(t)\rangle$, which represents EET among the initially excited donor and only those acceptors which are on neighboring polymer chains (or other types of chromophore aggregates such as micelles). This separation is mathematically rigorous in the context of the first-order cumulant approximation. Whether it is physically appropriate is an important question discussed in this work.

To calculate $\langle G^s_{\text{off}}(t)\rangle$ for chains of a given size with a specified number of chromophores, $\langle G^s(t)\rangle$ must be first calculated for an initially excited donor located on chain 1 and all possible configurations of chromophores on a second chain located a fixed distance, R_s, from chain 1 with no back-transfer (donor-trap, or DT EET). The two polymer chains are approximated by two Gaussian distributions of chromophores (Gaussian clouds) for the calculation of $G^s_{\text{off,DT}}(t)$. This is averaged over all possible initial positions on chain 1, yielding a single curve for a particular interchain distance R_s. This is repeated for a range of R_s. Since $\langle G^s_{\text{off,DT}}(t,R_s)\rangle$ will provide inputs for the subsequent calculation, it is necessary to choose a range of center-of-mass separations for the copolymer pairs from 0 to a distance large enough that there is no intercluster transfer, i.e., for which $\langle G^s_{\text{off,DT}}(t,R_s)\rangle = 1$ for all t under consideration. In practice, the maximum t is determined by the fluorescence lifetime, τ, of the chromophores. It is usually unnecessary to consider $t > 3\tau$.

The result is a distance-dependent $\langle G^s_{\text{off,DT}}(t,R_s)\rangle$ which describes the distance-dependent rate of transfer between two chains as if they were a pair of ''effective chromophores.'' The ensemble-average EET for a spatial distribution of any number of chains can then be calculated as the EET averaged over the spatial distribution of effective chromophores. This approach, developed by Marcus and Fayer,[5,6] is called the Effective Chromophore Method (ECM). For real chromophores, the Förster rate of transfer from chromophore 1 to chromophore 2 is $\omega_{12} = (1/\tau)(R_0/r_{12})^6$, where r_{12} is the chromophore separation. For N chromophores, this is the pairwise transfer rate that is used in the N coupled differential equations of the master equation. The N coupled equations must be ensemble-averaged over all possible spatial configurations of the N chromophores. The cumulant treatment is an approximate solution to the ensemble-averaged Master equation. Equation (1) contains the pairwise transfer rate in the exponential. In the ECM, $e^{-\omega_{12}t}$, the probability of finding the excitation on the initially excited chromophore

at time t,[30] should be replaced with the analogous probability of finding the excitation on the initially excited effective chromophore. As in the actual chromophore problem, this quantity reflects forward probability flow, without back-transfer. Therefore, it is the $G^s_{\mathrm{DT}}(t)$, the probability of finding the excitation on the initially excited cluster. In the limit that each cluster reduces to single chromophores each at a single location, $G^s_{\mathrm{DT}}(t)$ reduces to $e^{-\omega_{12}t}$. In the original treatment of the ECM, $G^s_{\mathrm{DD}}(t)$ was used rather than $G^s_{\mathrm{DT}}(t)$. $G^s_{\mathrm{DD}}(t)$ does not correspond to the pairwise transfer rate used for real chromophores because it includes back-transfer, and it does not reduce to $e^{-\omega_{12}t}$ when the clusters are reduced to single chromophores each at a single location.

To use the ECM to calculate the excitation transport observable for a system of clusters of chromophores, it is first necessary to calculate the DT EET between two clusters separated by a distance R_s. While straightforward in principle, the calculation can be a difficult problem in geometry because it is necessary to specify the distance between every chromophore on cluster 1 (the cluster containing the initially excited chromophore) and every chromophore on cluster 2 as a function of R_s, including distances for which the clusters may be interpenetrating. In the current work, it was found that the geometry relating the positions of chromophores in one cluster to those in another cluster was incorrectly simplified in Ref. 5, such that the set of distances between chromophores in different clusters was not fully represented in the resulting four-dimensional integral. A correct treatment of the geometry necessary to calculate intercluster EET is derived in Ref. 24. The final result of the derivation, a five-dimensional integral with the DT transfer rate, is given in the Appendix. The use of $G^s_{\mathrm{DD}}(t)$ and the four-dimensional integral to obtain the effective chromophore distance-dependent transfer probability in Ref. 5 gave rise to significant errors in the calculations of $\langle G^s_{\mathrm{off}}(t)\rangle$ in Refs. 6 and 17–20, although the errors tend somewhat to offset each other. Because Eq. (A1) is a five-dimensional integral, and because it is only necessary to calculate donor-trap EET to obtain $\langle G^s_{\mathrm{off,DT}}(t,R_s)\rangle$, it actually takes much less computer time to obtain $\langle G^s_{\mathrm{off,DT}}(t,R_s)\rangle$ by simulation than by numerical integration. MC simulations of intercluster DT EET are compared with Eq. (A1) in Ref. 24, demonstrating the perfect agreement that allows this time-saving substitution.

In the process of phase separation, copolymer molecules initially come together to form nanoscopic aggregates, or ''nanodomains.'' The copolymer molecules comprising these domains are represented by a distribution of effective chromophores, each located at the center-of-mass of the copolymer molecule it represents. EET among the effective chromophores in a nanodomain is then written in terms of

$$\langle G^s_{\mathrm{off}}(t,N_c)\rangle = \frac{1}{V}\int_{\mathrm{space}} \langle G^s_{\mathrm{off}}(t,N_c,\mathbf{r}_1)\rangle u(\mathbf{r}_1)d\mathbf{r}_1, \qquad (6a)$$

with

$$\langle G^s_{\mathrm{off}}(t,N_c,\mathbf{r}_1)\rangle = \exp\left(\frac{N_c-1}{2V}\int_{\mathrm{space}}[\langle G^s_{\mathrm{off,DT}}(t,R_s)\rangle^2-1]u(\mathbf{r}_2)d\mathbf{r}_2\right). \qquad (6b)$$

N_c is the number of chromophore-containing copolymer molecules in a nanodomain, and V is the nanodomain volume. The first integral [Eq. (6a)] is an average over all positions of a copolymer molecule bearing the initially excited chromophore, and the second integral [Eq. (6b)] is an average over all positions of a copolymer molecule bearing a chromophore which accepts an excitation. Equation (6) reduces to a three-dimensional integral, and the space can be described with spherical volume elements.

One simple model of a nanodomain is a random distribution of copolymer molecules within a spherical volume. For this distribution, interchain EET is described by

$$\langle G^s_{\mathrm{off}}(t,N_c)\rangle = \frac{3}{R^3_{\mathrm{dom}}}\int_0^{R_{\mathrm{dom}}} \exp\left(\frac{3(N_c-1)}{4R^3_{\mathrm{dom}}} \times \int_0^{R_{\mathrm{dom}}}\int_0^{\pi}[\langle G^s_{\mathrm{off,DT}}(t,R_s)\rangle^2-1]|r_2|^2 \times \sin\theta_2 dr_2 d\theta_2\right)|r_1|^2 dr_1, \qquad (7)$$

where R_{dom} is the nanodomain radius. The spherical volume has a hard cut-off. However, the effective chromophores represent Gaussian copolymer chains, and placing them in a sphere means placing the chains' centers-of-mass within a sphere. The distribution of chain segments extends beyond the sphere, falling off as a Gaussian from the surface.

III. NUMERICAL METHODS

Equations (2)–(4) and the analogous MC simulations are first computed to test the First-Order Truncated Cumulant Approximation; the results of these tests for Gaussian distributions and for uniformly filled spherical distributions with the donor at the center are presented to demonstrate the behavior of the theory independent of the polymer chain model. Then the single-chain theory for $\langle G^s_{\mathrm{on}}(t)\rangle$ [Eq. (5)] is compared to simulations of ensembles of random-flight polymer chains. Finally, EET in clusters of polymer chains is calculated using the ECM and compared with simulations.

A. Theory for intra- and interchain EET

Equations (2)–(5) and (7) are solved using numerical integration with either the Romberg or the Gaussian quadrature method[31] with abscissas at the zeros of the Legendre polynomial orthogonal to the weighting factors for Gaussian integration,[32] $P_{n=32}(x)$. Since most of the decay happens at early times, time steps of 0.05 ns are used from 0 to 15 ns, and time steps of 1 ns are used from 15 to 150 ns. For integrating uniform functions the Romberg method is used exclusively.

R_0 for an actual chromophore is scaled by the orientational parameter, γ, appropriate for the spatial dimensionality

of the system and the angular distribution of the chromophores in it.[30] In the glassy polymer systems discussed here, chromophore orientations are taken to be random and static, so $R_0' = \gamma^{1/3} R_0$, where $\gamma = 0.8452$. For chromophores inside a sphere, or effective chromophores in a spherical nanodomain, the upper limit on $|r|$ in Eqs. (3) and (7) is set equal to the sphere or nanodomain radius. The upper integration limit on $|r|$ in Eq. (2) is 5σ, and in Eq. (5) is $5 \times \langle R_g^2 \rangle^{1/2}$; increasing these respective limits to 10σ or $10 \times \langle R_g^2 \rangle^{1/2}$ does not change the results.

B. Monte Carlo simulations

The validity of the analytical EET theories is tested with MC simulations. The random numbers on which the simulations depend are prepared as follows: a seed number is passed to a random number generator[33] (rng) which selects 24 values which are in turn used as seeds for a rng using the algorithm of Marsaglia and Zaman,[34] which has a very large period ($\sim 10^8$) and passes the DIEHARD (Ref. 34) battery of statistical tests. 10 000 calls to this rng are made and discarded before proceeding with simulations, in order to reduce any bias that might arise from the 24 seed values. Subsequent calls result in a uniform distribution of values between 0 and 1. Output of the rng is either used directly, or this uniform distribution of random numbers is mapped onto a nonuniform distribution as needed.

Chromophores are assigned coordinates randomly within a sphere as follows. A uniform distribution in the radial coordinate is obtained by multiplying the cube of the radius by a random number, and taking the cube root of the result; this prevents over-sampling values of r which define a small volume, and under-sampling those which delimit a large volume. A random number is picked from 0 to 2π for the azimuth angle, and the value of the polar angle is found using $\theta = \mathrm{acos}(1-2F)$, where F is a random number in [0,1]. This weighting is needed to account for the fact that there is more volume into which the chromophore can be placed at the equator of the coordinate system than at the poles.[20] To obtain the coordinates of chromophores in a three-dimensional Gaussian cloud, a Gaussian distribution is randomly sampled along each of the Cartesian axes using the Box-Muller method.[31] Chromophore indices and coordinates are stored in a matrix, and the distances between them are calculated. An excluded volume parameter may be set so that if an overlap occurs, the entire chromophore configuration is discarded, and the chromophore placement process begins again.

When a nonoverlapping chromophore configuration has been found, a matrix of rate constants for EET between the chromophores is constructed. A standard Jacobi method[31] can be used to obtain the eigenvectors and eigenvalues of this real, symmetric matrix. For faster computation, the rate matrix is tridiagonalized using the Householder reduction method, and the QL algorithm with implicit shifts[31] is used to yield only the eigenvalues of the Pauli master equation, from which values of $\langle G^s(t) \rangle$ are determined.[20,35] This entire process is repeated and the results are averaged to yield $\langle G^s(t) \rangle$. Typically, $\langle G^s(t) \rangle$ converges after 5 000–10 000 repetitions.

When we wish to assign an excitation to a specific chromophore and watch the excitation hop from chromophore to chromophore in time, $\langle G^s(t) \rangle$ is determined differently. The following method is particularly useful for simulations of EET between chromophores in any of the configurations here described when the initially excited chromophore is always at a particular point in space, such as at the center of a uniform or Gaussian distribution, or on the end of a polymer chain. It is also used to check the results of simulations employing the matrix diagonalization formalism. Once the matrix of rate constants for excitation transfer between any two chromophores has been prepared, the sum of the rate constants for excitation transfer from the initially excited chromophore to all other chromophores is calculated and used to determine the probability of any transfer occurring during the first time step. Then a random number is chosen. If it exceeds the transfer probability, no transfer occurs, and the time is advanced. Otherwise, a new random number is chosen, and the rate of transfer from the excited chromophore to each other chromophore is summed in turn, until a chromophore whose rate constant has caused the sum to exceed the random number is reached. This chromophore accepts the excitation, and the probability of transfer from the newly excited chromophore to any other during the next time step is calculated. At each time step, the histogram slot assigned to that time step is incremented by 1 if an excitation was on the initially excited chromophore between its start and end times. The time is advanced, and this process is repeated until an entire decay of $G^s(t)$ from 0 to 2τ–10τ has been constructed. 10 000 or more decays are generated, and the average value in each histogram slot is reported as $\langle \underline{G}^s(t) \rangle$.

Freely jointed chains are modeled as arrays of N statistical segments of length a, which are set down as non-self-avoiding random walks in three dimensions. The first segment of a chain has one endpoint at the origin. To determine the position of its other endpoint in spherical polar coordinates, the radial coordinate is assigned the value a, and the azimuth and polar angles are chosen as described above. The endpoint of the first segment becomes the starting point of the next, until all the segments of a single chain have been placed in the coordinate system. The chain's center-of-mass is calculated, and moved to the origin. If the chain is to be placed in a nanodomain, it is instead moved to a randomly assigned position in the appropriate distribution about the origin.

Chromophores are now placed along the chain segments. A ''start'' segment is chosen at random, and the initially excited chromophore is placed at a random point on the line between that segment's endpoints. Each of the remaining chromophores is randomly assigned to any segment. The segments are then examined sequentially, and all of the chromophores that have been assigned to a segment but not yet placed on it are placed at random along a line between their segment's endpoints. If an overlap occurs, the entire chromophore configuration is discarded, and the chromophore placement process begins again with the empty chain. When a configuration has been found in which there occurs no overlap of chromophores on the same chain, the chromophore locations are written into a master matrix. If nan-

odomains are being simulated, additional chains are created, placed in the nanodomain, and given each a set of nonoverlapping chromophores whose locations are sequentially written into the matrix. If ever an overlap occurs between chromophores on different chains, the entire set of chains is discarded, and the process begins again with the construction of the first empty chain. A matrix of rate constants for EET between all of the chromophores is constructed from the distances calculated based on the master matrix of chromophore locations, and $\langle G^s(t)\rangle$ is determined as described above.

For comparison of Eq. (A1) with MC simulations, donor-trap versions of these simulations are used. Only one chromophore is placed in the initially excited chromophore's cluster so that no intracluster transfer can occur, and only one transfer event is allowed per configuration, because transfer from the initially excited donor to any other chromophore is irreversible.

Calculations and simulations were performed on IBM RS6000 Model 3BT and Powerstation 375 workstations, or an AS-ProDPSII workstation with dual Pentium II microprocessors. On the IBM workstations calculations of Eq. (5) for a copolymer with $N=10$ and $N=100$ out to 230 Å and three lifetimes (150 ns) with 436 time points as described above required 17.6 min, or 12.7 min on the AS-ProDPSII. Since the amount of time required for the calculation is directly proportional to the number and density of time points used, this run time can be shortened significantly. The amount of time required for MC simulations is very sensitive to N, N, the excluded volume parameter, and the number of time steps. Obtaining $\langle G^s_{\mathrm{on}}(t)\rangle$ for the same parameters with time steps of 0.05 ns by MC simulation required 53 min for the hopping simulation, but only 9.6 min for the matrix-reduction method. The density of time points is constant in the simulations, but can be varied (e.g., increased for short times) in the calculations. Because of the simplicity of the DT simulation and the complexity of Eq. (A1), it is much quicker to obtain $\langle G^s_{\mathrm{off,DT}}(t,R_s)\rangle$ by MC simulation than by performing the five numerical integrations involved in the analytical calculation. However, once $\langle G^s_{\mathrm{off,DT}}(t,R_s)\rangle$ has been obtained, it can be much quicker to obtain the total $\langle G^s(t)\rangle$ for multiple chains using Eq. (7) instead of MC simulations of EET on multiple chains. For example, for copolymer molecules with $\langle R_g^2\rangle^{1/2}=34$ Å and $N=36$, MC simulations have taken 1–2 h for nanodomains composed of two chains ($N_c=2$), 11–12 h for nanodomains with $N_c=7$, and 21–22 h for $N_c=10$, while calculations of Eq. (7) take several minutes with run times independent of N_c.

IV. RESULTS AND DISCUSSION

A. Tests of the cumulant approximation

Since ensembles of single polymeric molecules are modeled as Gaussian distributions of chain segments, the theory for the simpler restricted geometry of chromophores distributed randomly in a Gaussian cloud is compared with MC simulations before examining the behavior of the theory for EET on a polymer chain. In Fig. 1, calculation of $\langle G^s(t)\rangle$ for chromophores in Gaussian clouds with no constraints on the position of the initially excited chromophore [Eq. (2)] are compared to simulations for the fixed volume of a three-dimensional Gaussian distribution, $(2\pi\sigma^2/3)^{3/2}$, for a variety of number densities, ρ. $\rho=3N/4\pi r^3$, corresponding to the reduced concentrations $C=(4\pi/3)R_0^3\rho$. N is shown below the decays. Experiments on polymers have used naphthalene chromophores with $R_0\cong 13$ Å, which is used here. The standard deviation of the Gaussian ($\sigma=34.25$ Å) is comparable to the root-mean-square radius of gyration, $\langle R_g^2\rangle^{1/2}$, of a moderate molecular weight polymer chain. As is clear from the figure, agreement between theory and simulation is very good for Gaussians with only 2 chromophores ($C=0.25$) to those containing a reduced concentration of 8.00. That the theory with the first-order truncated cumulant approximation can describe the complex process of excitation transfer in finite volumes over such a range of concentrations so well is impressive, especially considering its simplicity and ease of use.

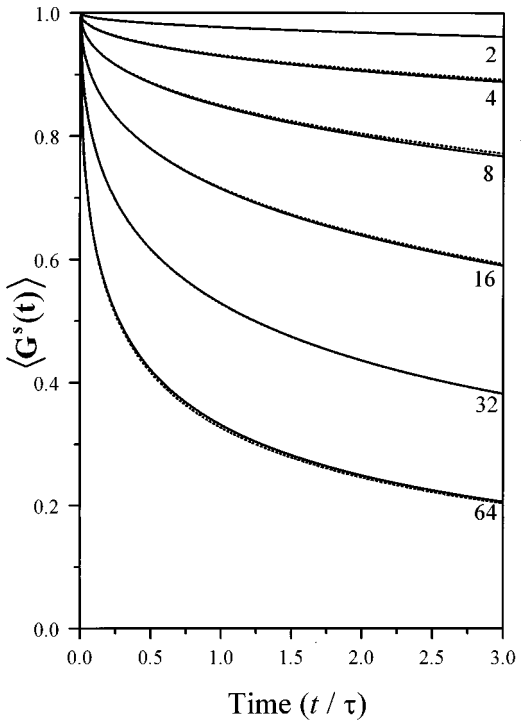

FIG. 1. $\langle G^s(t)\rangle$ calculated for Eq. (2) (dashed lines) and simulated (solid lines) for chromophores in three-dimensional Gaussian clouds of increasing density. N, the number of chromophores in the Gaussian volume, is shown below the corresponding curves.

Results for spheres whose volume and densities match those of the clouds in Fig. 1 are given in Ref. 24. They also demonstrate excellent agreement between theory and simulations at all chromophore concentrations. Comparing $\langle G^s(t)\rangle$ for matched densities reveals that the decays for the spherical volume are faster than those for the Gaussian volume. Although the concentration peaks at the center of a Gaussian volume, the influence of the increased local concentration near the center is reduced by the small r^2dr volume element there. Because the Gaussian extends well beyond the hard cutoff of the sphere, there are many configurations of chromophores which are more widely separated than in the spherical volume. These configurations are important in the ensemble average, slowing the overall rate

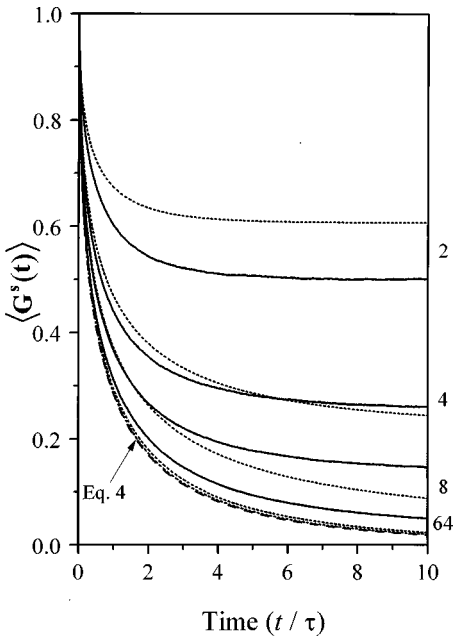

FIG. 2. Calculations (dashed lines) and simulations (solid lines) of $\langle G^s(t) \rangle$ for a series of spheres with constant density but increasing size [Eq. (3)], demonstrating convergence to Eq. (4). $\bar{C}=1$. At small N, the effect of the incorrect asymptotic behavior of the theoretical calculation is strongest; when the sphere radius approaches $6\times R_0$, the excitation that began at its center no longer shows the effects of encountering the edge of the distribution, and the calculations for the spheres converge to that for the infinite-solution limit.

of excitation transfer in a Gaussian compared to that in a sphere of the same volume.

Under a variety of circumstances, the cumulant approximation does not behave as well as in the situation shown in Fig. 1. Figure 2 displays results of calculations and simulations in which the initially excited chromophore is fixed at the center of a sphere [Eq. (3)] and the other chromophores are distributed randomly. The figure shows a comparison for a series of spheres with constant density ($\bar{C}=1.0$) but increasing size. Also shown is the calculation of $\langle G^s(t) \rangle$ for a random distribution of chromophores in an infinite solution [Eq. (4)]. The infinite solution result has been demonstrated to be very accurate.[9] Because the initially excited chromophore is fixed at the center, the average distance between it and other chromophores is smaller than for the case in which the initially excited chromophore can be located anywhere in the sphere. Thus, the concentration is effectively higher than in a randomly distributed system with the same $\bar{C}$.

The curves in Fig. 2 go out to 10τ. While measurements of such a long decay are experimentally unrealizable, these results provide insight into the source of error in the cumulant approximation. At small N, the effect of the incorrect asymptotic behavior in the theoretical calculation of $\langle G^s(t) \rangle$, which was recognized by Peterson and Fayer,[4] is strongest; the calculated curve for $N=2$ reaches 0.6067 by 10τ, while the simulation reaches the correct probability of 0.5000 by 8τ. As the sphere becomes larger with respect to R_0 and N increases, agreement between theory and simulation improves for times up to 2τ, the time scale of experimental interest. Even with the initially excited chromophore fixed at the center of the sphere, once there are 4 or more chromophores, the cumulant approximation does a reasonable job and converges to the infinite solution limit as the volume and the number of chromophores increase. Therefore, the behavior of the model for $t>2\tau$ does not compromise its usefulness in analyzing experimental data. However, the failure of the cumulant approximation to go to the correct asymptotic limit is still evident at long time. The cumulant calculations approach a value, $\exp[(1-N)/2]$, that is smaller than the correct asymptotic limit, $1/N$, so the calculations begin to fall below the simulations. This behavior is evident in the $N=4$ and $N=8$ curves.

When the sphere becomes very large, N becomes so large that the asymptotic limit becomes indistinguishable from zero in either the exact calculation or the cumulant approximation. The infinite-order theory of Gochanour, Andersen, and Fayer (GAF) (Ref. 9) for infinite solutions [Eq. (4)] was also tested with simulations by Engström *et al.*,[36] who found excellent agreement when they used periodic boundary conditions and the minimum image convention in their simulations. However, if they used a simple spherical volume, they found discrepancies. The simulations conducted in this study for very large spheres show discrepancies identical to those of Engström *et al.* Since this study is focused on the behavior of the theory and simulations for finite-volume systems, the necessary procedures to make the simulations converge for an infinite system were not implemented. Analysis of Gaussians with the initially excited chromophore at the center gives similar results.[24]

B. Theory and simulations of EET on polymer chains

1. Intramolecular EET

Freely jointed chains have an ensemble-average spatial distribution which is approximately Gaussian. However, there are important differences between a freely jointed chain model and a Gaussian cloud. The coordinates of points in the cloud are independent, i.e., the location of one chromophore does not change the probability distribution for another chromophore. However, for a chain, the upper limit on the distance between the chain's end points means that the combination of the squares of any two chromophores' coordinates cannot exceed the square of the length of the stretched chain. Thus, the Gaussian chain-segment density distribution is more compact than the Gaussian cloud with the same σ, so that $\langle G^s(t) \rangle$ for the chain will decay more quickly than $\langle G^s(t) \rangle$ for the cloud. Furthermore, as discussed below, there are significant correlations among the locations of chromophores on a chain which do not exist for a cloud. Comparisons of simulations of EET on chains with simulations and cumulant calculations for the Gaussian cloud distribution confirm that the differences between the two spatial distributions of chromophores are significant.[24]

The distribution function given in Eq. (5c) was employed to describe the spatial distributions of chromophores on a polymer chain. Equation (5c) is based on the probability function for finding a particular segment j a distance r away from the segment i, which contains the initially excited chro-

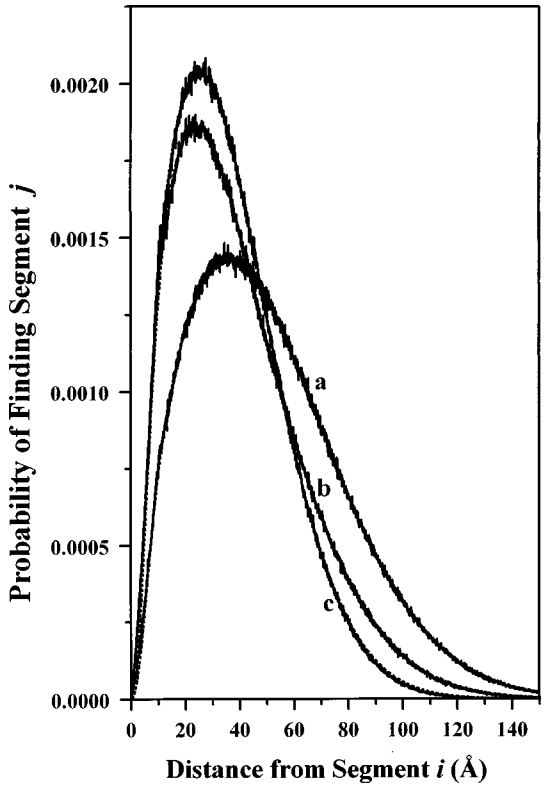

FIG. 3. The probability of finding a segment j a distance x from a given segment i for a chain of 55 segments, from Eq. (5c) (dashed lines) and simulations (solid lines). (a) $i=1$ (end segment); (b) $i=14$; (c) $i=28$ (middle segment). The agreement is almost perfect, so that over most of the range the lines are indistinguishable.

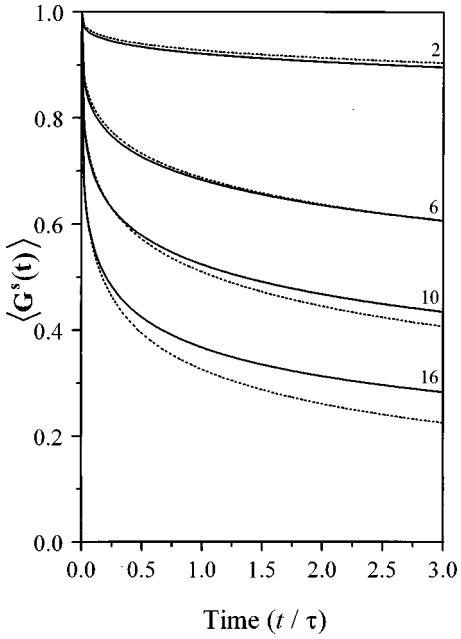

FIG. 4. Calculations (dashed lines) and simulations (solid lines) of EET on polymer chains with 55 statistical segments of length 11.2 Å [Eq. (5)]. The root-mean-square radius of gyration of this molecule is 33.9 Å; N, the number of chromophores on a chain, is shown above the curves. The agreement is very good, but the accuracy decreases as N increases. For $N=16$, the error corresponds to ~3 Å error in the determination of $\langle R_g^2\rangle^{1/2}$.

mophore. A sum is then performed over all j to give the probability of finding any segment a distance r away from the initially excited segment i. An average is also performed over i [Eq. (5)].

To determine whether the non-self-avoiding random walk used to model the chain for the MC simulations of EET corresponds to the chain-segment density distribution function used in the EET calculations, profiles of the probability of finding chain segments at various distances from a particular segment i were constructed both from simulations and Eq. (5c). Figure 3 displays the results. The calculations are for a 55 segment chain, with $i=1$, 14, and 28. These are pair correlation functions. Since the chromophores are on the chain segments, the distributions represent the probability of finding a chromophore a distance r away from the initially excited chromophore on the ith segment. The agreement between the simulated and calculated distribution functions is essentially perfect. Therefore, any differences between the EET simulations and calculations do not arise from differences in the *pairwise* spatial distribution of chromophores.

For the comparison between the cumulant theory and the simulations, specific parameters were selected to resemble those that have been used in previously reported experiments.[16] The experiments involved copolymerization of methylmethacrylate and a small amount of 2-vinylnaphthalene which yielded polymers of polymethylmethacrylate (PMMA) lightly tagged with naphthalene chromophores. Small amounts of the tagged PMMA were homogeneously mixed with optically inert host polymers and annealed to form composite glasses. The copolymer guest behaved as if in θ-conditions when blended with a PMMA host, and collapsed in an incompatible polyvinylacetate (PVAc) host. The statistical segment length used for the copolymer in PVAc is $a=11.2$ Å; the model chain is composed of 55 statistical segments, and its $\langle R_g^2\rangle^{1/2}=33.9$ Å. The chromophore distribution used in the theory places the initially excited chromophore at the center of a statistical segment. For comparison, the initially excited chromophore was also placed at the center of the segment in the simulations. Whether the initially excited chromophore is placed at the midpoint of its segment or randomly along it makes negligible difference in simulations of $\langle G^s(t)\rangle$.

Figure 4 displays the results of the cumulant calculations and the simulations for several choices of N, the number of chromophores per chain. When N (the tagging fraction) is not too large, the agreement is excellent. Similar results were obtained for a variety of chain sizes. The agreement between theory and simulation is clearly not as good as for the curves displayed in Fig. 1, which shows results for chromophores randomly distributed in a Gaussian cloud. However, if the $\langle R_g^2\rangle^{1/2}$ in the theory is used as an adjustable parameter and fit to the simulated curve for $N=16$, the $\langle R_g^2\rangle^{1/2}$ needs to be increased by ~3 Å to bring the curves into good agreement. Thus, even for a high tagging fraction, the error is not great.

The reduction in the accuracy of the chain calculations compared to the simulations does not arise from the incorrect asymptotic behavior of the cumulant theory, since none of the decays are displayed at long enough times to be approaching the asymptotic limit of $1/N$; the extent of the decays toward their asymptotic limits is similar to that in the

sphere and Gaussian cloud calculations for which there are virtually no deviations between theory and simulation. Furthermore, as shown in Fig. 3, the pair distribution functions used in the cumulant calculations and the simulations are essentially identical.

The reduced quality of the agreement for the polymer chain when N is large can be attributed to the correlations that exist among chain segments, and the fact that the cumulant theory is sensitive only to the pair correlation function and not to higher-order correlations. In the Gaussian cloud, the location of one chromophore does not influence the possible locations of other chromophores. For a chain with chromophores on its segments, the chromophores have the same correlations as the segments. These correlations go beyond pair correlations. Chain configurations can produce clusters of neighboring chromophores. An excitation can leave the initially excited chromophore, loop through two or three other chromophores and return to the initially excited chromophore. The first-order cumulant approximation does not account for such paths. These paths are not of great importance when the chromophore concentration is low, and they play almost no role when the chromophore locations are not highly correlated.

An important consideration in designing polarization experiments is that the orientational distribution of the chromophores must be known. The easiest way to meet this stipulation is to ensure that their orientational distribution is random. This requires that there be fewer than one chromophore per statistical segment of the copolymer. As N increases it becomes less likely that this stipulation is met. Thus, we find that for parameters that are appropriate for experiment, agreement between theory and simulation is quite good. For the range of tagging fractions that is useful in experiments, the cumulant theory is capable of providing an accurate determination of $\langle R_g^2 \rangle^{1/2}$. The accuracy has been tested experimentally[15] and shown to be very good.

2. Intermolecular EET

Extension of the theory to EET between the chromophores on different copolymer chains depends upon the combined utility of the cumulant approximation and the Effective Chromophore Method. The ECM depends on the separability of $\langle G^s(t) \rangle$ into contributions to the total EET from excitation transfers among chromophores on the same chain and contributions from transfers among chromophores on different molecules, i.e., $\langle G^s(t) \rangle = \langle G^s_{\rm on}(t) \rangle \langle G^s_{\rm off}(t) \rangle$. Because the cumulant expansion is truncated at first order (a pair approximation), the separation is formally allowed. However, the question is open as to how accurate the analytical treatment is.

The Peterson and Fayer calculation provides $\langle G^s_{\rm on}(t) \rangle$, which, as shown above, provides an accurate description of transfer on a single chain under the proper conditions. $\langle G^s_{\rm off}(t) \rangle$ is obtained using the ECM with Eq. (7) as described above.

Figure 5 shows the results of calculations of $\langle G^s(t) \rangle$ for ensembles of spherical nanodomains. The onset of phase-separation is modeled as spinodal decomposition, in which nanodomains (with radius equal to $\langle R_g^2 \rangle^{1/2}$ of the guest copolymer) maintain a constant volume, while the density of guest copolymer inside them increases. Curves (a) present $\langle G^s_{\rm on}(t) \rangle$ for single guest copolymer chains of molecular weight 55 000 with 10 chromophores per chain. Curves (b) are calculations and simulations of EET for nanodomains containing two of these chains ($N_c = 2$), and curves (c) show the same for $N_c = 7$. The agreement between theory and simulation is reasonable, demonstrating that the theory, which depends upon the first-order cumulant approximation, the separability of $\langle G^s_{\rm on}(t) \rangle$ and $\langle G^s_{\rm off}(t) \rangle$ and on the effective chromophore method, is a good description of EET among chromophore-bearing polymers. Given the number of approximations in the analytical theory, the results are remarkable. While the quality of the agreement varies, similar agreement can be found for a variety of domain sizes and chain sizes.

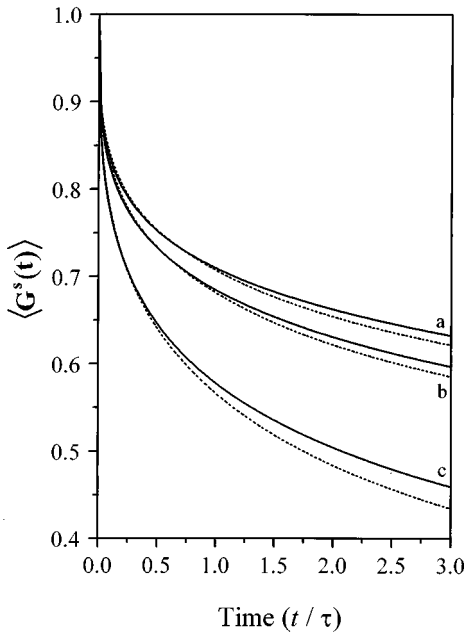

FIG. 5. Calculations (dashed lines) and simulations (solid lines) of (a) Eq. (5) for copolymers with $N = 10$ and $\bar{N} = 122$; (b) Eq. (7) for an ensemble of spherical domains containing 2 such copolymer chains, and (c) Eq. (7) for domains of the same size, each containing 7 chains.

Curves (a) demonstrate that the intrachain EET theory with the cumulant approximation works well for this system. In the interchain EET theory, polymer molecules are modeled not as chains of statistical segments, but as Gaussian clouds. Chains are more compact than clouds. This means that EET for isolated clouds is slower than that for isolated chains, but also that there is significant overlap between clouds for a greater range of R_s than for chains.[24] These differences may give rise to the differences between simulation and theory shown in curves (b) and (c). Unlike simulations of nanodomains with large numbers of chains, the analytical theory is rapidly implemented on a fast workstation for any number of chains. Therefore, it can be used to fit experimental data, providing a powerful method for the study of nanophase separation.

The theory is also useful in optimizing experimental design. We can examine various combinations of parameters

and predict the time-resolved anisotropy decays for the polymer systems they represent. For this case we find that the growth of nanodomains from $N_c=2$ to $N_c=7$ will be detectable for a number of chromophores, N, that is low enough to be appropriate for measuring $\langle G^s_{\rm on}(t)\rangle$. Furthermore, just as the desire for a random orientational distribution stipulates that N be small, the densities of polymeric materials under study place an upper bound on N_c. The range of N_c in Fig. 5 is that allowed for polymers of 55 000 molecular weight and bulk density 1.19 g/cm^3, modeled after common polymers. The change in the observable is large enough to monitor nanodomain formation in experimental systems of guest polymers of this molecular weight. If the range of physically allowed N_c for a particular composite material is broad enough that a distribution in N_c should be considered, it is straightforward to weight the contributions to the observable from nanodomains with different N_c accordingly. We have examined a Poisson distribution in N_c with a weighting by the number of chromophores per nanodomain, since those with more chromophores are more likely to capture an excitation and subsequently contribute to $\langle G^s(t)\rangle$. Such treatment further reduces the differences between theoretical and simulated decays. If the disagreement is large, the simulations are still very useful for data analysis.

V. CONCLUDING REMARKS

We have shown that the MC simulations for EET in polymer systems compares favorably with previously developed analytical theory, demonstrating excellent agreement in the realm of experimentally appropriate parameters. Lowering the reduced concentration, which slows the approach to the asymptotic limit, diminishes the discrepancies between theory and simulation. The reduced concentration can be lowered by decreasing N, and also by decreasing $R_0/r_{\rm sphere}$. Since decreasing N maximizes the difference between $\exp[(1-N)/2]$ and $1/N$, decreasing $R_0/r_{\rm sphere}$ does the most to improve agreement. This can be achieved by selecting a chromophore with an appropriate value of R_0. The distinction between small N and low reduced concentration is therefore important to bear in mind in the process of experimental design.

The discrepancies between simulation and theory that are large generally occur for situations that fall outside the combined range of parameters for experimental tractability or prudent design, e.g., at long times and high N. This is also the case when higher-order terms not contained in the first-order cumulant approximation can contribute significantly to the description of EET on polymer chains. Situations for which agreement is compromised are readily identifiable. For volumes which are small with respect to R_0, exactly how large or small N can become if the theory is to be useful for interpreting experimental data can be determined by looking at calculations and simulations for the set of parameters in question. For analysis of data from phase-separating polymer blends, nanodomain size and shape can be varied to fit $\langle G^s(t)\rangle$ to experimental data. The net result is that the theory is well suited for analysis of experimental data. The calculations are significantly more efficient than simulations for fitting data from systems with large numbers of chains.

ACKNOWLEDGMENTS

We thank Professor Binny Cherayil, Department of Inorganic and Physical Chemistry, Indian Institute, Bangalore, India for helpful discussions. This work was supported by the Department of Energy, Office of Basic Energy Sciences (Grant No. DE-FG03-84ER13251). S.M. acknowledges support from the Swiss National Science Foundation.

APPENDIX

The general form and derivation of $\langle G^s_{\rm off,DT}(t,R_s)\rangle$ for donor-trap EET between an initially excited donor in one chromophore cluster and a group of $N-1$ chromophores in a different cluster is presented in Ref. 24, which includes figures detailing the correct coordinate system for describing intercluster transfer. For the specific case of EET between chromophores on copolymer molecules modeled as Gaussian distributions of polymer segments,

$$\begin{aligned}\langle G^s_{\rm off,DT}(t,R_s)\rangle &= 2\pi\left(\frac{3}{2\pi\langle R_g^2\rangle}\right)^{3/2}\int_0^{r\max}\int_0^{\pi}\left[\left(\frac{3}{2\pi\langle R_g^2\rangle}\right)^{3/2}\right.\\ &\times\exp\left(\frac{-3r_1^2}{2\langle R_g^2\rangle}\right)\int_0^{r\max}\int_0^{\pi}\int_0^{2\pi}\exp\left(\frac{-3r_2^2}{2\langle R_g^2\rangle}\right)\\ &\times\left.\exp\left[\left(\frac{-t}{\tau}\right)\left(\frac{R_0}{r_{12}}\right)^6\right]r_2^2 dr_2\,\sin\,\theta_2 d\theta_2 d\varphi_2\right]^{N-1}\\ &\times r_1^2 dr_1\,\sin\,\theta_1 d\theta_1. \qquad \text{(A1)}\end{aligned}$$

In brief, $0\leqslant\theta_i\leqslant\pi$, measured from the positive half of the z-axis for each cluster. The separation between the clusters' centers-of-mass lies along the z-axis. $0\leqslant\varphi_i\leqslant 2\pi$, which is in cluster i's xy-plane and measured from its positive x-axis, and $0\leqslant r_i\leqslant\infty$, measured from the origin of cluster i.

[1] *Polymer Blends and Alloys*, edited by P. S. Hope and M. J. Folkes (Blackie, London, 1993).
[2] O. Olabisi, L. M. Robeson, and M. T. Shaw, *Polymer–Polymer Miscibility* (Academic, New York, 1979).
[3] *Polymer Blends*, edited by D. R. Paul and S. Newman (Academic, New York, 1978).
[4] K. A. Peterson and M. D. Fayer, J. Chem. Phys. **85**, 4702 (1986).
[5] A. H. Marcus and M. D. Fayer, J. Chem. Phys. **94**, 5622 (1991).
[6] A. H. Marcus, N. A. Diachun, and M. D. Fayer, Macromolecules **26**, 3041 (1993).
[7] D. M. Hussey, L. Keller, and M. D. Fayer, Mol. Cryst. Liq. Cryst. **283**, 173 (1996).
[8] L. Keller, D. M. Hussey, and M. D. Fayer, J. Phys. Chem. **100**, 10257 (1996).
[9] C. R. Gochanour, H. C. Andersen, and M. D. Fayer, J. Chem. Phys. **70**, 4254 (1979).
[10] S. W. Haan and R. Zwanzig, J. Chem. Phys. **68**, 1879 (1978).
[11] M. D. Ediger and M. D. Fayer, J. Chem. Phys. **78**, 2518 (1983).
[12] D. L. Huber, Phys. Rev. B **20**, 2307 (1979); **20**, 5333 (1979).
[13] A. Blumen, J. Chem. Phys. **72**, 2632 (1980).
[14] M. D. Ediger, R. P. Domingue, and M. D. Fayer, J. Chem. Phys. **80**, 1246 (1984).
[15] K. A. Peterson, M. B. Zimmt, S. Linse, R. P. Domingue, and M. D. Fayer, Macromolecules **20**, 168 (1987).
[16] K. A. Peterson, A. D. Stein, and M. D. Fayer, Macromolecules **23**, 111 (1990).

[17] A. H. Marcus, M. D. Fayer, and J. G. Curro, J. Chem. Phys. **100**, 9156 (1994).
[18] A. H. Marcus, D. M. Hussey, N. A. Diachun, and M. D. Fayer, J. Chem. Phys. **103**, 8189 (1995).
[19] A. H. Marcus, N. A. Diachun, and M. D. Fayer, J. Phys. Chem. **96**, 8930 (1992).
[20] K. U. Finger, A. H. Marcus, and M. D. Fayer, J. Chem. Phys. **100**, 271 (1994).
[21] Th. Förster, Ann. Phys. (Leipzig) **2**, 55 (1948); Z. Naturforsch. A **4**, 321 (1949).
[22] C. R. Gochanour and M. D. Fayer, J. Phys. Chem. **85**, 1989 (1981).
[23] M. D. Ediger, R. P. Domingue, K. A. Peterson, and M. D. Fayer, Macromolecules **18**, 1182 (1985).
[24] D. M. Hussey, Ph.D. thesis, Stanford University, 1998.
[25] G. H. Fredrickson, H. C. Andersen, and C. W. Frank, J. Polym. Sci., Polym. Phys. Ed. **23**, 591 (1985).
[26] A typographical error in Ref. 4 gives an incorrect factor of $2^{3/5}$ in place of $2^{1/2}$.
[27] H. Yamakawa, *Modern Theory of Polymer Solutions* (Harper & Row, New York, 1971).
[28] W. Kuhn, Kolloid-Z. **76**, 258 (1936); **87**, 3 (1939).
[29] M. Kurata and Y. Tsunashima, in *Polymer Handbook*, 3rd ed. (Wiley, New York, 1989).
[30] J. Baumann and M. D. Fayer, J. Chem. Phys. **85**, 4087 (1986).
[31] W. H. Press, S. A. Teukolsky, W. T. Vetterling, and B. P. Flannery, *Numerical Recipes in C: The Art of Scientific Computing*, 2nd ed. (Cambridge, New York, 1992).
[32] M. Abramowitz and A. Stegun, *Handbook of Mathematical Functions, with Formulas, Graphs, and Mathematical Tables* (Dover, New York, 1965).
[33] F. James, Comput. Phys. Commun. **60**, 329 (1990).
[34] G. Marsaglia, and A. Zaman, Ann. Appl. Prob. **1**, 462 (1991).
[35] J. D. Byers, W. S. Parsons, R. A. Friesner, and S. E. Webber, Macromolecules **23**, 4835 (1990).
[36] S. Engström, M. Lindberg, and L. B.-Å. Johansson, J. Chem. Phys. **89**, 204 (1988).